Revised Manuscript

This is the accepted version of the publication Norouzi M, Sajjadi Alehashem SM, Vatandoost H, Ni YQ, Shahmardan MM, A new approach for modeling of magnetorheological elastomers, Journal of Intelligent Material Systems and Structures (Vol.27 and Issue No. 8) pp. 1121-1135.
 DOI: 10.1177/1045389X15615966

A new approach for modeling of magneto-rheological elastomers

Mahmoud Norouzi[1], Seyed Masoud Sajjadi Alehashem[2], Hossein Vatandoost[1], Yi Qing Ni[3] and M. M. Shahmardan[1]

[1]Department of Mechanical Engineering, Shahrood University of Technology, Shahrood, Iran.
[2]Department of Civil Engineering, Kharazmi University, Karaj Campus, Iran.
[3]Department of Civil and Environmental Engineering, The Hong Kong Polytechnic University, Hung Hom, Kowloon, Hong Kong, China.

Corresponding author:

Mahmood Norouzi, [1]Department of Mechanical Engineering, Shahrood University of Technology, Shahrood, Iran.
Email: mnorouzi@shahroodut.ac.ir

Abstract

This paper presents a novel model to portray the behavior of magneto-rheological elastomer (MRE) in oscillatory shear test. Dynamic behavior of an isotropic MRE is experimentally investigated at different input conditions. A modified Kelvin-Voigt viscoelastic model is developed to describe relationships between shear stress and shear strain of MREs based on input frequency, shear strain and magnetic flux density. Unlike the previous models of MREs, the coefficients of this model, calculated by nonlinear regression method, are constant at various harmonic shear loads and different magnetic flux densities. The results show that the new phenomenological model can effectively predict the viscoelastic behavior of MREs. Also, the results demonstrate that the trend of shear storage modulus of MRE based on the frequency is nonlinear from 0.1 Hz to 8 Hz, which is predicted by the present model. The proposed model is beneficial to simulate vibration control strategies in MRE base devices under harmonic shear loadings.

Keywords: Magneto-rheological elastomer, modeling, viscoelastic, Kelvin-Voigt model.

Introduction

Magneto-rheological (MR) materials, such as MR fluid, MR foam and MR elastomer are a kind of smart material its rheological properties are proportional to the external magnetic field. MR materials are fabricated by embedding micron-sized magnetizable particles in a non-magnetic matrix such as fluid, gel or rubber like materials. MR elastomers are solid analogues of MR fluid that the magnetizable particles can be distributed homogeneously (Isotropic MRE) or to be formed such a chain-like columnar structures (Anisotropic MRE) in a matrix. Their rheological properties can be controlled by an applied external magnetic field. The fabrication of these two kinds of MREs is depended on whether the external magnetic field is applied or not during MRE curing process (Carlson and Jolly, 2000; Chen et al., 2007; Li et al., 2013b; Ying et al., 2013; Li et al., 2014). The mechanical properties and MR effect of both isotropic and anisotropic MREs with and without external magnetic field is studied and a reversible change in modulus with external magnetic field is observed. It was found that the stiffness and damping properties of anisotropic MREs depend on the mutual directions of load, magnetic field and the particles alignment in the composite (Kallio, 2005).

MRE magnetic field dependent modulus merits it to being flexible and controllable so that sustain large deformation in tension, compression and shear mode. Unlike to MR fluid, sedimentation of magnetizable particles, liquid leakage and environmental contamination not happen in MRE due to solid like matrix. Additionally, there is no need

a container to hold MR materials in place. The response time of MREs, which is about few milliseconds, is less than MR fluids due to particles lock in place in solid like matrix, so no need time for particles to be rearranged in presence of magnetic field. MR fluids have field dependent yield stress and variable damping and typically operate in a post-yield continuous shear flow regime while MREs normally operate in the pre-yield regime (Chen et al., 2008; Gong et al., 2005; Li and Zhang, 2008; Zhang et al., 2008). This makes the two branches of materials complementary rather than competitive to each other. At this case, MR fluid-elastomers (MRFEs) are used in a variety of devices such as helicopter lag dampers, MRFE mounts and MRFE isolators. Despite of all mentioned facts, MR fluids have a widespread use in mitigating vibration and controlling devices and have more effective output force than MREs (HU and WERELEY, 2005; Kallio, 2005; Ngatu et al., 2010; 2012; York et al., 2007). MR fluids have been used in damping devices (Yang et al., 2002), particularly dampers in bridges (Gordaninejad et al., 1998) and suspension systems (Raja et al., 2010), rotary actuators (Guo and Liao, 2012), clutches (Kavlicoglu et al., 2002), MR seat suspension system (Bai and Wereley, 2014) and brakes (Wang et al., 2005). On the other hand, MREs are used in adaptive tuned vibration absorber (Deng et al., 2006; Sun et al., 2014; Zhang, 2009), adaptive isolators (Li et al., 2013c), variable stiffness and damping isolators (Behrooz et al., 2014b), vehicle seat suspension (Du et al., 2011), micro cantilevers (Dongkyu et al., 2014), force sensor (Li et al., 2009), actuators (Zhou and Wang, 2005), noise barrier systems (Farshad and Le Roux, 2004), sandwich beams (Hu et al., 2011) and negative changing stiffness isolators (Yang et al.,

2014). An adaptive tuned vibration absorber that can shift its natural frequency from 75 Hz to 150 Hz is developed (Zhang, 2009). The MRE devices can forcibly put an end to seismic hazards and keep away from the system resonance response if the appropriate control strategy is considered. These applications can be controlled by active, passive or semi-active strategy. Most of researchers focus on semi-active strategy because of its less power consumption relative to active devices and its flexible controllability over passive systems (Behrooz et al., 2014a; Du et al., 2011).

Modeling and understanding dynamic behavior of MREs under various loading conditions is essential to design appropriate MRE-based devices for vibration control. Up to now, MRE modeling is considered in two different viewpoints; micro model aspect and macro model aspect. The micro model aspect has two branches. The first branch of micro model aspect is based on continuum mechanics. At these models, the finite strain theory is used in order to study of coupled mechanical and magnetic behavior of MREs. These models consider the impact of shape, orientation, distributions, chain-like structures and size of magnetically susceptible particles on stress components (Danas et al., 2012; Galipeau and Ponte Castañeda, 2013).The second branch of micro model aspect is micro mechanical-based; typically focus on studying and modeling field dependency of modulus, MR effect and stress specifically in shear mode. This branch is based on interaction of dipole magnetic particles of particles chain .Researchers have been used a wide variety of simplified assumptions about the local strain and magnetization field (Davis, 1999; Shen et al., 2004).

The macro model aspect is based on the relation of force-displacement or stress-strain of MREs in different modes, particularly shear mode and compression mode, including viscoelastic and mathematical approach. These models are more practical than the micro model aspect because of capability to capture the MRE-based devices behavior and simply be prepared for simulation and vibration control design. The rheological properties of MRE in addition to the magnetic field, is depended on magnitude and frequency of strain, which is shown in our research experimentally. At this case, other experiments indicated this dependency (Blom and Kari, 2005; Stepanov et al., 2007; Wu et al., 2010; Zhou, 2003).

The beneficial and executable control simulation for MRE-based devices should be regardless of the loading condition. Consequently, the comprehensive model should consider all loading conditions such as input frequency, strain and magnetic field intensity in order to cover all dynamic performance of MRE. Up to now, different models are proposed to simulate MRE behavior. A four-parameter linear viscoelastic model that its coefficients in addition to the magnetic field are slightly strain dependent is presented by Li et al. (2010). Zhu et al. (2012) proposed a four-parameter viscoelastic fractional derivative model. The proposed model parameters are frequency independent, working at different frequency from 1 Hz to 10 Hz, while they are strain-dependent. The nonlinear spring element represents the magnetic-field dependency. Eem et al. (2012) developed a dynamic model combining the Ramberg-Osgood model and Maxwell model with four magnetic-field dependent parameters and one constant coefficient. However, its

parameters are independent of strain and input frequency while Ramberg-Osgood model gives the strain in terms of stress and that an explicit equation cannot be derived for the stress in terms of strain. A nonlinear constitutive model depending on applied magnetic field and strain and frequency is proposed by Blom and Kari (2011). The viscoelastic and frictional part of this model needs a time-consuming task to be calculated. This model is suitable for modeling of MRE-device applications that working in high frequency ranges such as engine mounts and bushings.

Furthermore, MREs and MRE isolators exhibit typical hysteresis behavior, specifically in large amplitude excitation. This nonlinear hysteresis behavior typically is represented by Bouc-Wen model (Wen, 1976) that is very well accepted. However, one of the main problems of Bouc-Wen hysteresis model is estimating of its seven model parameters and specifically including evolutionary variable that caused the parameter identification requiring great computational resources. Moreover, the parameters of Bouc-Wen model at most of the former studies are frequency dependent and strain dependent. The contribution of frequency in non-linearity of the hysteresis loop of force-displacement may not be as important as strain or applied magnetic field, but in order to reach a comprehensive and accurate model it should be considered. Yu et al. (2014a) used a hyperbolic element instead of Bouc-Wen model to model the hysteresis behavior of MRE isolator. The parameters of this model is frequency dependent. Behrooz et al. (2014a) employed a model consisting Bouc-Wen element in order to characterize the force-displacement relationship of MRE isolator that its parameters are frequency and

strain dependence. Yang et al. (2013) proposed a model for MRE isolator based on Bouc-Wen model that can effectively predict nonlinearity due to ascending strain. In this model, the influence of each magnetic-field dependent parameter on the shape of the hysteresis loop completely studied. However, these parameters are strain and frequency dependent that means it is essential to implement an optimization process at different loading condition each time. Li and Li (2013) exerted another phenomenological model with strain dependent and frequency dependent parameters based on Koh-Kelly model. Yu et al. (2014b) proposed a strain-stiffening model for MRE isolator by using non-linear strain stiffening spring (power low function). Getting the proposed model parameters are not easy to be searched by attempts due to differential equations and need to implement minimization optimization.

In this paper, the complexity and shortcoming in common models are resolved. At first step, the viscoelastic properties of MREs in shear mode are experimentally investigated. Dynamic hysteresis loops as well as the dependence of dynamic shear storage modulus (G') and loss factor (ζ) of MRE upon the loading frequency, strain and magnetic flux density are experimentally obtained. The second part focused on developing a dynamic model for MRE that can accurately predict its behavior regarding the effect of magnetic field, strain and frequency, concurrently. Therefore, by implementing this heuristic model, there is no need to solve any differential equation or run optimization process every time to updated model's parameters with respect to different loading conditions. Additionally, the proposed model could precisely estimate the behavior of shear storage

modulus (G') based on the frequency in a wide range from 0.1 Hz to 8 Hz, which is nonlinear while the previous works of MREs only predicted the linear behavior of shear storage modulus (G') based on the frequency especially from 1 Hz to 10 Hz.

Experimental setup

The tested MRE is an isotropic MRE, which contains carbonyl iron particles (type C3518, Sigma-Aldrich), silicone rubber (Silicone sealant, Selleys) and silicone oil (type 378364, Sigma-Aldrich). The weight fraction of carbonyl iron particle, silicone rubber, and silicone oil are 70%, 20% and 10%, respectively. The diameter range of iron particles is from 3 μm to 5 μm, which are dispersed in the silicon matrix randomly. Each MRE specimen has a dimension of 50×12×9.5 mm. As shown in Figure 1. A specific fixture is designed for the experiment. The fixture consists of two steel plates that are made of steel and fixed together in a specific distance by using four stainless steel screws and bushings. The distance between the two plates is set according to the total thickness of the MRE specimens and the sandwiched plate between them. The permanent magnets are installed on the fixture to induce magnetic field perpendicular to the plane of shear force direction. Changing the numbers of the installed permanent magnets enables to vary the magnetic field that passes uniformly through the MRE specimens.

The experiment is conducted with a servo-hydraulic material testing machine as shown in Figure 2 that operates in displacement-control mode under harmonic excitations with

different combinations of strains and frequencies. Different magnetic flux densities are provided by permanent magnets. The loading frequencies are f=0.1, 0.3, 0.5, 1, 3, 5, 8 Hz and the displacement amplitudes are A=0.19, 0.38, 0.76, 1.52 mm that correspond to shear strain amplitudes for the specimens with 9.5 mm thickness being γ_0=2%, 4%, 8%, 16%, respectively. The magnitude of the flux density is varied from B=0 mT (no magnet installed) to B=100, 180, 230 and 272 mT for investigating the effect of magnetic field on dynamic behavior of the MRE.

Experimental results and discussion

Hysteresis loops

Hysteresis loops of tested MRE under different strains and frequencies are shown in Figures 3 and 4 when magnetic flux density is B=0 mT (without magnet) and B=272 mT (with 4 magnets), respectively. These Figures illustrate the effect of strain on the shape of hysteresis loop in different input frequencies. It is evidence that MRE shows a symmetric behavior with an elliptical shape in shear mode in both situations with and without an applied magnetic field. For the same strain and the same frequency, the captured area of hysteresis loops (that indicates the dissipated energy in each cycle or equivalent damping) for an applied magnetic field is larger than those obtained without applied magnetic field. Moreover, MRE response stress (for the same strain and the same frequency) for the applied magnetic field situation is greater. In addition, applying

magnetic field increases the slope of hysteresis loops that characterizes the equivalent stiffness of the MRE. Specially, the slope increment with the applied magnetic field is more evident in small strain. The hysteresis loops are also affected by the input frequency. Figure 5 illustrates the effects of frequency on shape of the hysteresis loop with same strain for magnetic flux density B=0 mT and B=272 mT. It is obvious that the slope of hysteresis loops as well as captured area of each loop is increased by increasing input frequency in both situations with and without applied magnetic field. However, this increment for applied magnetic field situation is more evident (Figure 5(b)). In order to show the effect of magnetic field in MRE behavior, the typical stress-strain response of harmonic shear deformation at constant frequency and strain for different levels of applied magnetic field from B=0 mT to B=272 mT are shown in Figure 6. As can be seen, for all cases, by increasing magnetic flux density the shape of loops are changed in which the slope of the hysteresis loops are increased and the area enclosed by the loops is enlarged that means the dissipated energy per cycle by MRE is enhanced.

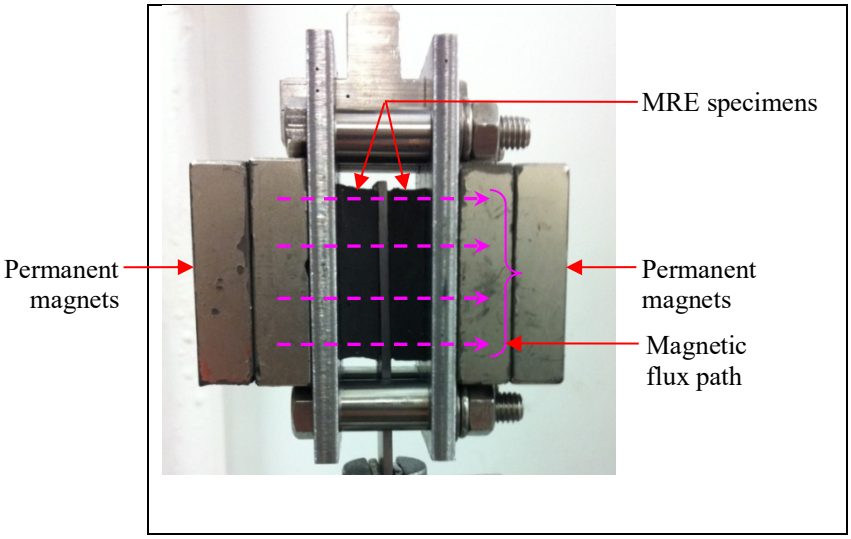

Figure 1. Fixture with MRE specimens and permanent magnets installed on it.

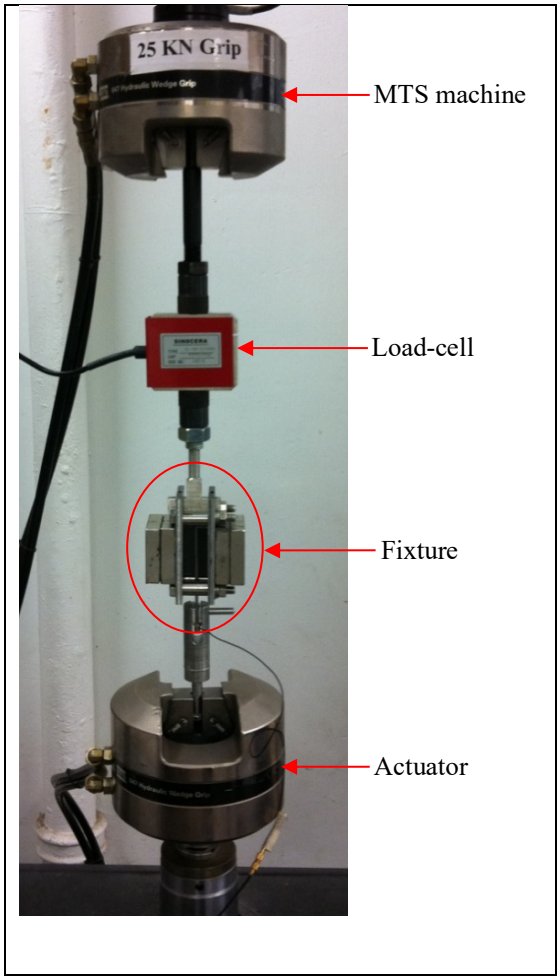

Figure 2. Experiment on material testing machine.

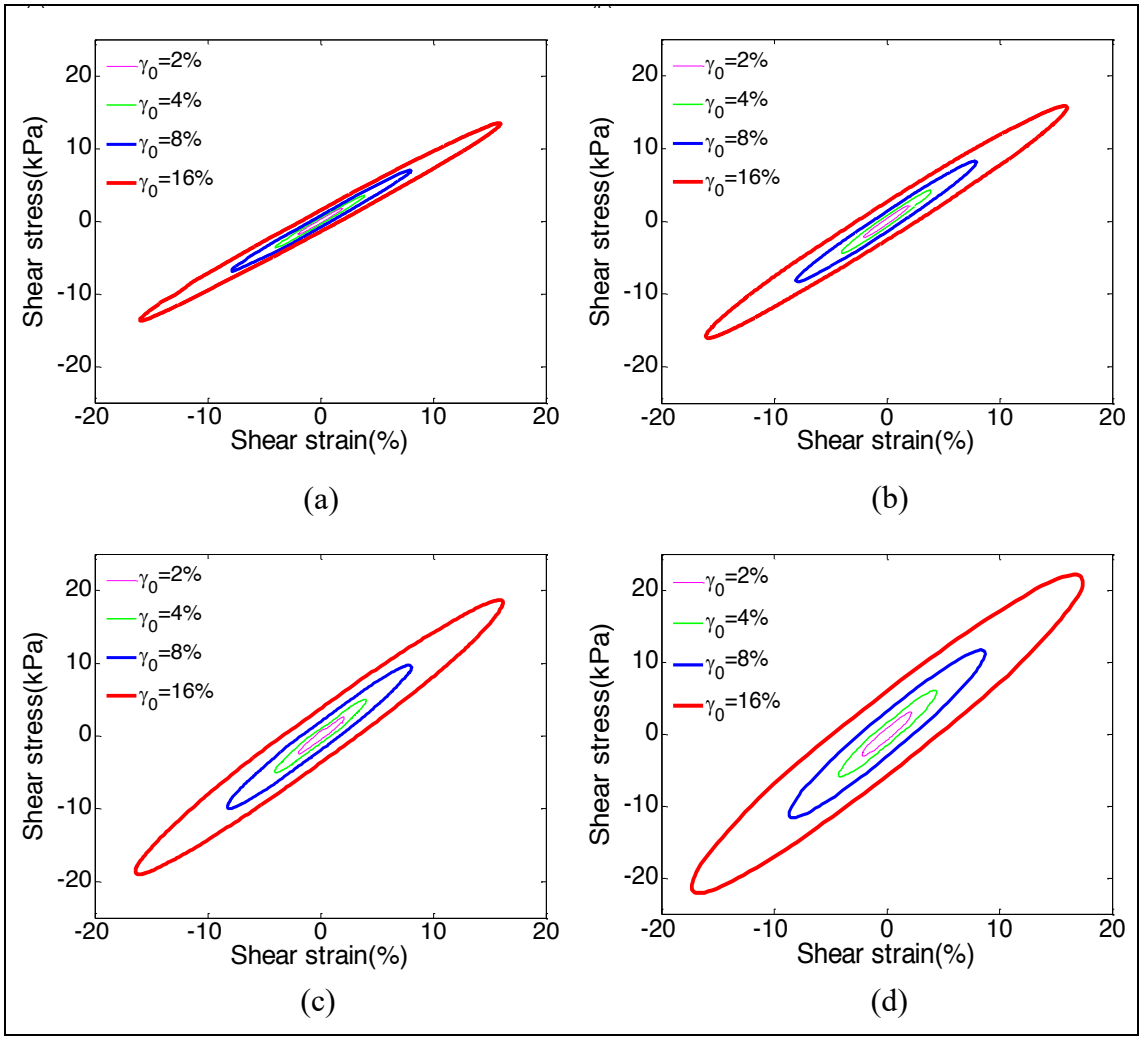

Figure 3. Hysteresis loops with magnetic flux density B=0 mT (without magnetic field). (a) f=0.1 Hz, (b) f=1 Hz, (c) f=3 Hz, (d) f=8 Hz.

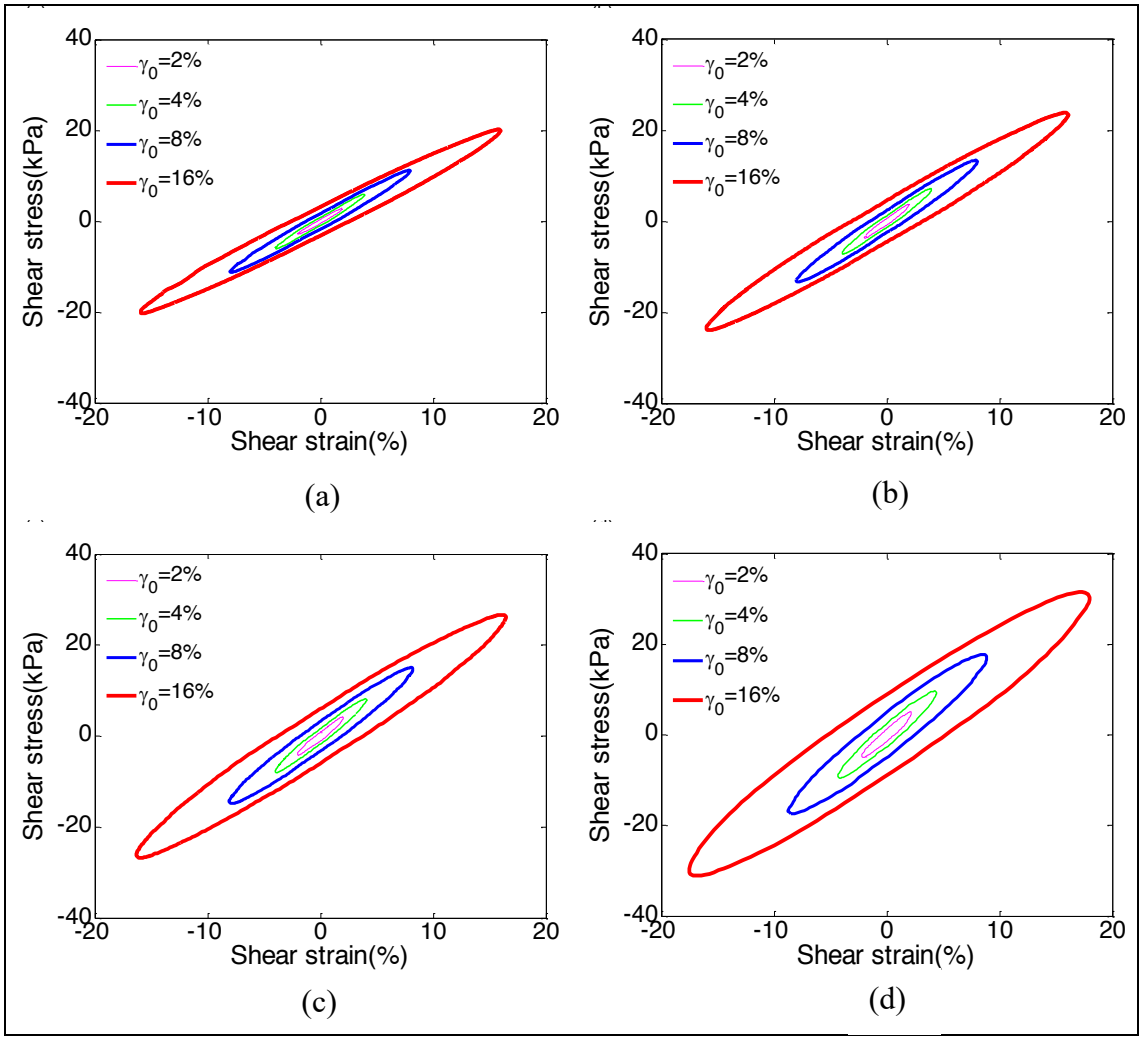

Figure 4. Hysteresis loops with magnetic flux density *B*=272 mT.
(a) *f*=0.1 Hz, (b) *f*=1 Hz, (c) *f*=3 Hz, (d) *f*=8 Hz.

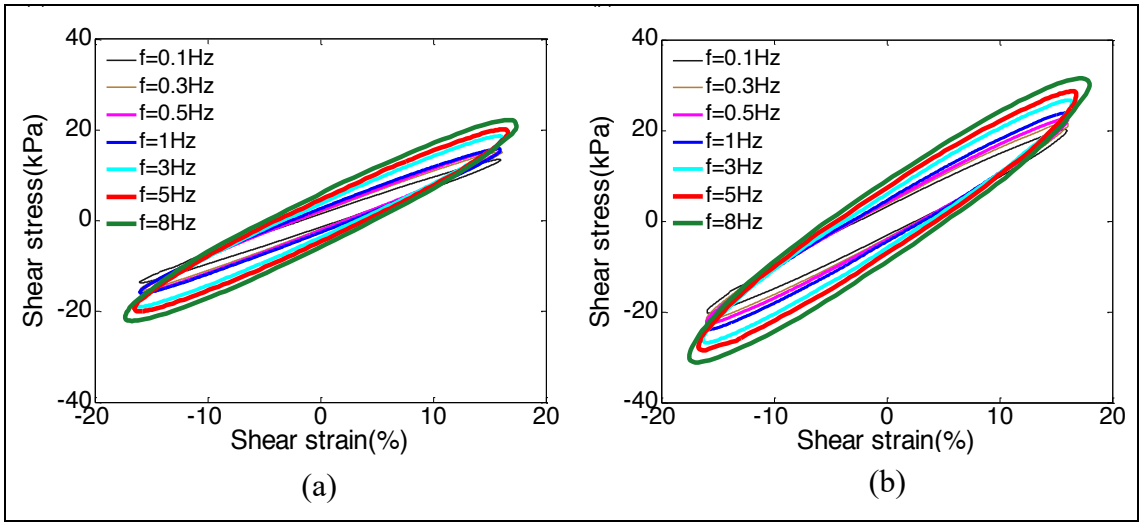

Figure 5. Hysteresis loops under different frequencies with strain γ_0=16%.
(a) Magnetic flux density *B*=0 mT, (b) Magnetic flux density *B*=272 mT.

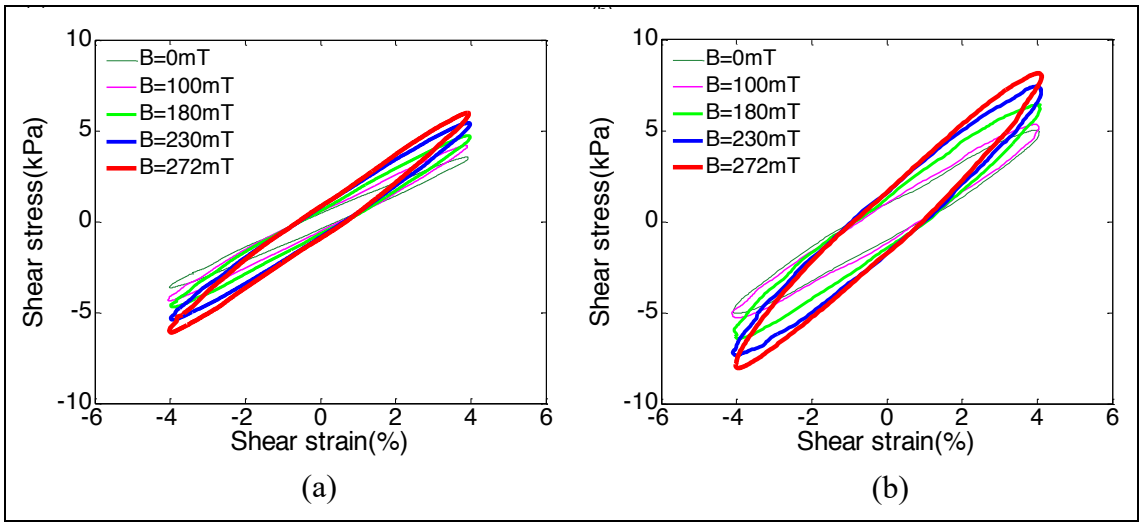

Figure 6. Stress-strain response under different levels of magnetic flux density with strain γ_0=4%.
(a) f=0.1 Hz*, (b) f*=3 Hz.

Magnetic field dependence of MRE properties

In order to quantitatively characterizing the effect of applied magnetic field on MRE properties, the magnetic field dependence of storage modulus and loss factor is shown in Figures 7 and 8, respectively. As shown in Figure 7, shear storage modulus (G') is enhanced quadratically by increasing magnetic flux density in all input frequencies for all tested shear strains. The trend of increment is quite same over the range of tested frequencies with this distinctive that for higher input frequency the level of (G') is larger and by increasing input frequency the curves are shifted to higher values. Moreover, the increment is more remarkable in smaller strain that already observed in hysteresis loops of the MRE. Figure 8 shows the trend of change in loss factor versus magnetic flux density for different input frequencies and shear strains. It is found that the loss factor increases almost linearly by increasing magnetic flux density. This increment is more remarkable in larger shear strain.

Frequency dependence of MRE properties

The properties of MREs in addition to deformation (strain) are depended upon the rate of deformation (strain-rate dependent).The variation of shear storage modulus versus input frequency for different magnetic flux densities are shown in Figure 9. It is observed that the shear storage modulus increases by increasing input frequency. In other words, the MRE shows strain-rate stiffening effect. However, the slope of increment is not uniform and varies by the input frequency. The variation of (G') can be divided into two zones;

frequencies smaller than 1 Hz and frequency higher than 1 Hz. Therein, the shear storage modulus shows an exponentially increment up to frequency f=1 Hz. Beyond the 1 Hz, (G') increase almost linearly by increasing the input frequency. In the general form, it can be concluded that the shear storage modulus of MRE is a power function of frequency with the positive power of less than one. However, most studies of MRE were done in frequency higher than 1 Hz and therefore the reported relation of (G') in term of frequency is linear (Gong et al., 2005; Kallio et al., 2007; Lokander and Stenberg, 2003; Wang et al., 2007). Figure 10 shows the variation of loss factor versus frequency for different magnetic flux densities. With the same manner of the (G'), loss factor ζ shows different variation in frequencies lower and higher than 1 Hz. The loss factor increases almost linearly in frequencies higher than 1 Hz, whereas for frequency lower than 1 Hz, the trend of increment is faster and it almost increases exponentially.

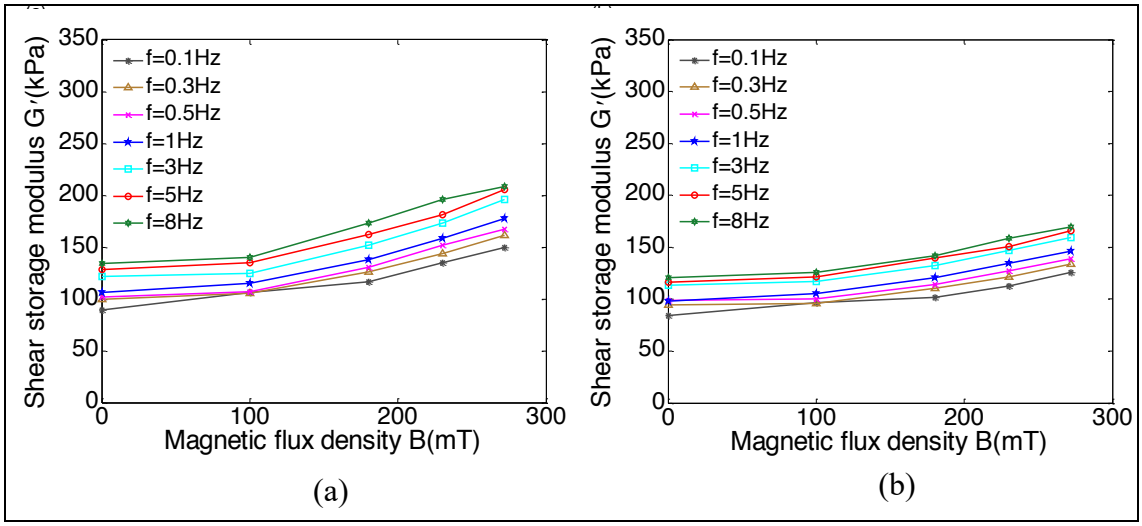

Figure 7. Shear storage modulus versus magnetic flux density for different input frequencies. (a) γ_0=4%, (b) γ_0=16%.

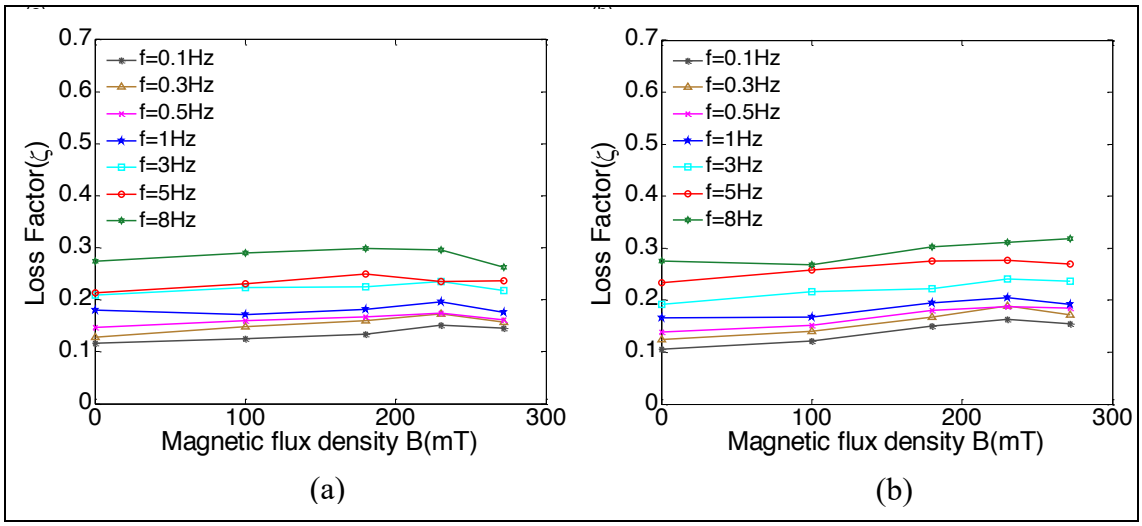

Figure 8. Loss factor versus magnetic flux density for different input frequencies. (a) γ_0=4%, (b) γ_0 =16%.

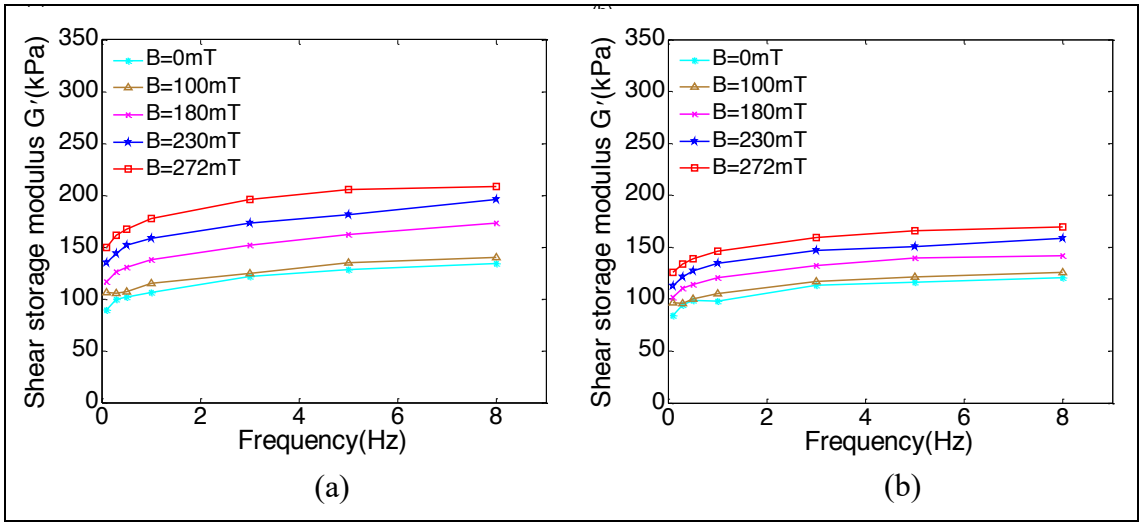

Figure 9. Shear storage modulus versus frequency for different magnetic flux densities. (a) γ_0=4%, (b) γ_0=16%.

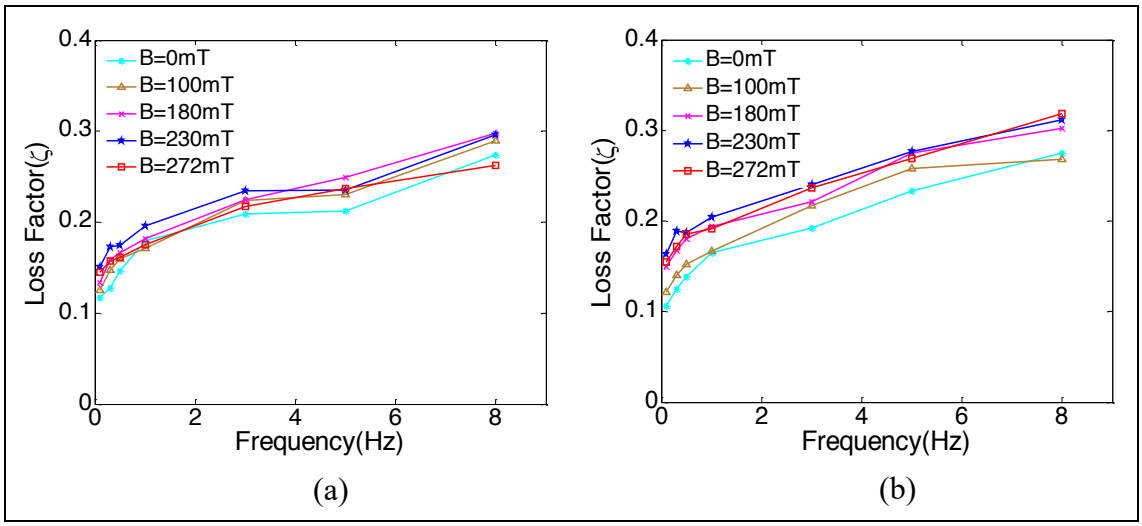

Figure 10. Loss factor versus frequency for different magnetic flux densities. (a) γ_0=4%, (b) γ_0=16%.

Displacement dependence of MRE properties

In absence of a magnetic field, due to viscoelastic nature of elastomer, another feature of MRE is apparent which is referred to Flether-Gent effect (W.P. Fletcher, 1953) also known as Payne effect (Payne and Whittaker, 1971). This phenomenon is defined as the decrease of shear storage modulus with increasing amplitude of oscillation (Leblanc, 2002; Payne and Whittaker, 1971). At the specific applied magnetic field by increasing the strain, the magnetic force between magnetic particles, which are embedded in the matrix, becomes less. Hence, by increasing strain the shear modulus of MRE is decreased as shown in experimental results. In other words, the MRE shows strain softening behavior. Additionally, based on the Figure 4 by increasing the strain the slope of main axis is slightly reduced. This reduction is referred to strain softening effect, which is appeared in linear regime (perfect elliptical-shape loops are apparent in stress-strain curves). Figure 11 shows the effect of strain in MRE storage modulus for different levels of magnetic flux density. By increasing strain, the storage modulus reduces approximately linearly for all tested frequencies. This reduction in (G') is steeper for higher magnetic field levels. As shown in Figure 11, for B=0 mT (without magnetic field) the shear storage modulus is not changed as that much and it is almost constant. The reduction of shear storage modulus by increasing strain is due to magnetic forces between magnetic particles in MRE matrix that has conversely dependence with particles distance. Figure 12 shows the effect of strain in loss factor of MRE for different levels of magnetic

flux density. It is found that the loss factor is independent of strain and it does not change effectively by increasing strain.

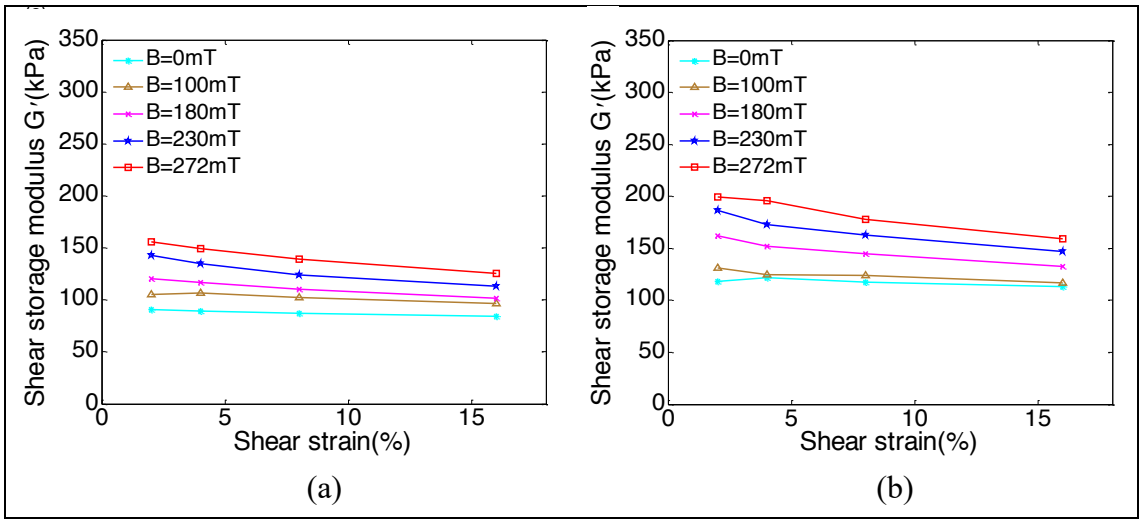

Figure 11. Shear storage modulus versus strain for different magnetic flux densities.(a) *f*=0.1 Hz, (b) *f*=3 Hz.

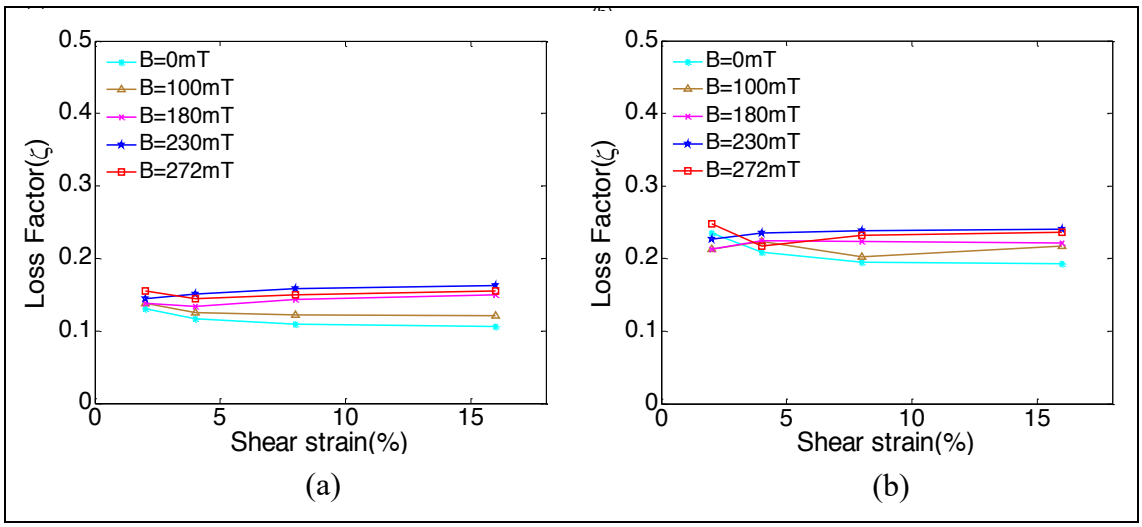

Figure 12. Loss factor versus strain for different magnetic flux densities. (a) *f*=0.1 Hz, (b) *f*=3 Hz.

MRE modeling

Mathematical model

Based on the experimental results, the viscoelastic property of MRE in addition to the external magnetic field is depended on loading conditions. For all loading conditions at different magnetic flux densities, the force-displacement curves indicate perfect elliptical-shape. In order to predict the response of MRE, a mathematical model based on viscoelastic Kelvin-Voigt model is adopted, as shown in Figure 13. As stiffness and damping of MRE are depended on external magnetic field, loading frequency and strain, these dependencies should be represented in model. Based on the results, the frequency dependency with MRE stiffness and damping is represented by a power function. The strain dependency with MRE stiffness is represented by a power function whereas MRE damping is almost steady by varying strain. Finally, the magnetic-field dependency with MRE stiffness and damping is represented by a polynomial function.

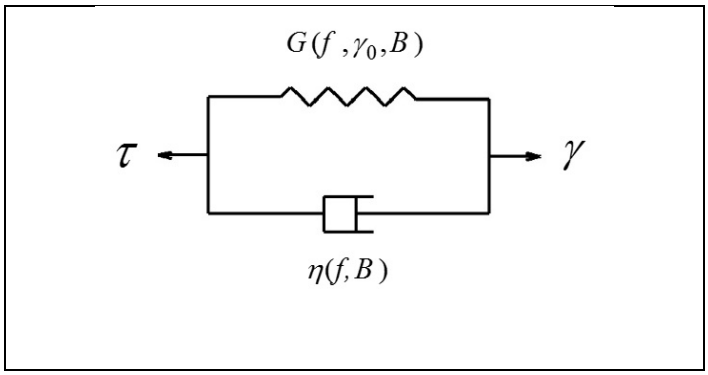

Figure 13. Modified viscoelastic Kelvin-Voigt model for MREs.

In this model $G(f,\gamma_0,B)$ and $\eta(f,B)$ are shear storage modulus and viscosity, respectively that their behavior are resembled to the stiffness and damping. Additionally, f , f_0, γ_0 and B are loading frequency, reference frequency of 1 Hz, strain amplitude and magnetic flux density, respectively. The stress-strain relationship is given as below.

$$\tau(t) = G(f,\gamma_0,B)\,\gamma(t) + \eta(f,B)\dot{\gamma}(t) \quad (1)$$

where $\tau(t)$ and $\gamma(t)$ are stress output and strain input. Suppose that the shear strain input $\gamma(t)$ is a harmonic excitation.

$$\gamma(t) = \gamma_0 \sin(2\pi f\, t) \quad (2)$$

In conventional viscoelastic Kelvin-Voigt model, the shear storage modulus (G) and viscosity (η) are constant. While in proposed model shear storage modulus (G) and viscosity (η) are represented as below.

$$G(f,\gamma_0,B) = a_B \left(\frac{f}{f_0}\right)^{b} (\gamma_0)^{c_B} \quad (3)$$

$$\eta(f,B) = d_B \left(\frac{f}{f_0}\right)^{e} \quad (4)$$

Suppose that the input complex strain is γ^* and shear complex modulus is G^*, the complex shear stress τ^* can be given by

$$\tau^* = G^*\gamma^* = (G' + iG'')\gamma^* \quad (5)$$

Then suppose that

$$\gamma^{*} = \gamma_0 e^{i\omega t} \tag{6}$$

where G^{*}, G' and G'' are shear complex modulus, shear storage modulus and shear loss modulus respectively. By substituting equations (5) and (6) into (1), the G' and G'' can be expressed as

$$G' = a_B \left(\frac{f}{f_0}\right)^{\mathrm{b}} (\gamma_0)^{c_B} \tag{7}$$

$$G'' = 2\pi d_B \left(\frac{f}{f_0}\right)^{1+\mathrm{e}} \tag{8}$$

In addition, the loss factor can be calculated as

$$\zeta = \frac{G''}{G'} = \frac{2\pi d_B \left(\frac{f}{f_0}\right)^{(\mathrm{e}-\mathrm{b}+1)}}{a_B (\gamma_0)^{c_B}} \tag{9}$$

Parameter Identification

The developed viscoelastic model consist five parameters, i.e. a_B, b, c_B, d_B and e. The proposed model uses shear strain as an input and then calculates the shear storage modulus $G(f, \gamma_0, B)$ and viscosity $\eta(f, B)$ that required for the model. Afterward, gives the shear stress determined by equation (1). Five parameters are calculated by implementing the nonlinear regression algorithm in order to minimize the error between experimental stress τ_{Exp} and model-predicted stress τ_{Model} for each external magnetic

field. The difference between model and experiment is represented by fitness function error as below.

$$ff = \sum_{i=1}^{N}\sum_{j=1}^{M}(\tau_{Model}(i,j) - \tau_{Exp}(i,j))^2 \qquad (10)$$

where N and M are the number of different experimental data of shear loading conditions, frequency and strain, respectively. This optimization is done at different magnetic fields. These parameters are calculated and are presented in Table 1. From this table, it is found that the parameters a, c and d are magnetic field dependent whereas the parameters b and e are constant by varying magnetic field. By increasing the applied magnetic field, parameters a_B and d_B are increased quadratically while c_B is increased steadily. At this case, a nonlinear curve fit was implemented to these three parameters.

Table 1. Parameters used for phenomenological model.

Magnetic field (mT)	a_B (kPa)	b	c_B	d_B (kPa.s)	e
0	94.9956	0.09504	-0.0143	2.7917	-0.6410
100	96.0495	0.09504	-0.0430	2.9170	-0.6410
180	104.6167	0.09504	-0.0700	3.5417	-0.6410
230	112.0370	0.09504	-0.0995	4.2083	-0.6410
272	120.3517	0.09504	-0.1010	4.3750	-0.6410

The magnetic-field dependent parameters are calculated and listed in Table 2. Furthermore, the three polynomial functions are determined from nonlinear curve fit that is explained as below.

$$a_B = a_{B_2} B^2 + a_{B_1} B + a_{B_0} \quad (11)$$

$$c_B = c_{B_1} B + c_{B_0} \quad (12)$$

$$d_B = d_{B_2} B^2 + d_{B_1} B + d_{B_0} \quad (13)$$

Table 2. Constant coefficients used for functions of magnetic field**.**

Parameter	Value
$a_{B_2}\,(\mathrm{kPa}/(\mathrm{mT})^2)$	4.582×10^{-4}
$a_{B_1}\,(\mathrm{kPa}/\mathrm{mT})$	-3.067×10^{-2}
$a_{B_0}\,(\mathrm{kPa})$	94.869
$d_{B_2}\,(\mathrm{kPa.s}/(\mathrm{mT})^2)$	2.179×10^{-5}
$d_{B_1}\,(\mathrm{kPa.s}/\mathrm{mT})$	4.766×10^{-4}
$d_{B_0}\,(\mathrm{kPa.s})$	2.7544
$c_{B_1}\,(1/\mathrm{mT})$	-3.403×10^{-4}
c_{B_0}	-1.233×10^{-2}

Comparison between experimental results and Model estimation

In this study, four levels for strain, seven levels for input frequency and five levels for magnetic field is utilized. Totally, 140 sets of experimental data are gathered as stress-strain loops that can be modeled only by ten constant parameters. Eight of constants are

listed in Table 2 and two constants, b and e, are presented in Table 1. By using the constant parameters from system identification methodology, the comparison of experimental results and model prediction is shown in Figure 14 to 19. Figure 14 shows the stress-strain relationship of MRE at different strains. It can be seen from the Figures that the model prediction is fitted perfectly to experimntal results and strain softening effect is accurately captured by proposed model. Based on the Figure 14(a) the strain-softening effect becomes more obvious at the high frequency and also for higher magnetic flux densities. Additionally, the area of hysteresis loops is increased by increasing the strain, which is predicted by proposed model very well. As shown in Figure 15, the model pridection is completely in accordance with experimental results and strain-rate stiffening is captured by the proposed model, properly. Figure 16 shows the effect of magnetic field on mechanical properties of MREs that is also appropriately predicted by proposed model. It can be seen from the Figures that by increasing the external magnetic field, the slopes of main axis and area of hysteresis loops are ascending that are precisely captured by proposed model.

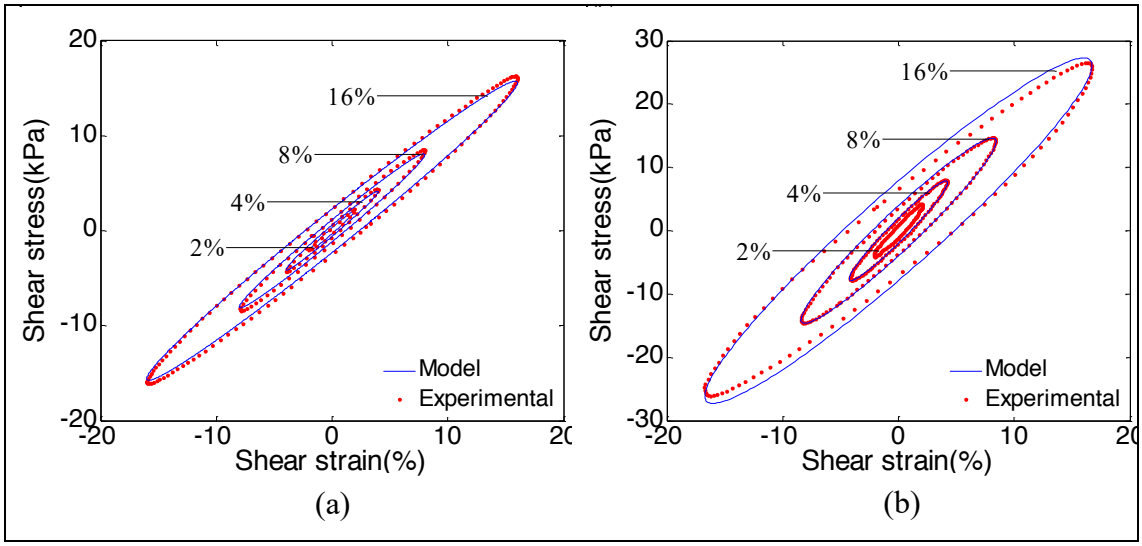

Figure 14. The stress-strain curves of experimental data and proposed model for different strains. (a) B=100 mT and f=0.5 Hz, (b) B=230 mT and f=5 Hz.

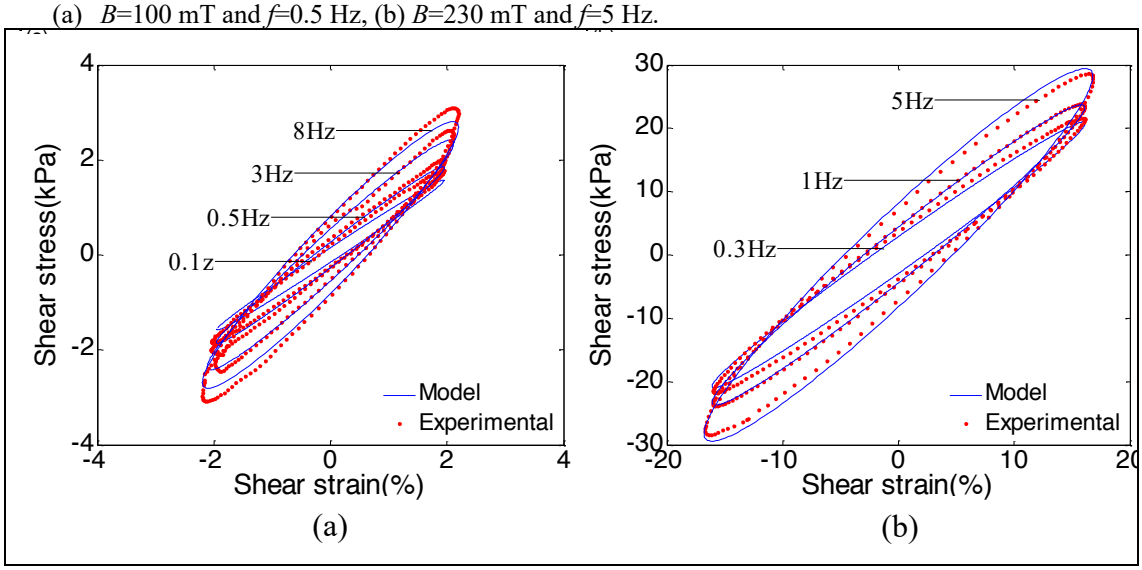

Figure 15. The stress-strain curves of experimental data and proposed model for different input frequencies. (a) γ_0=2% and B=0 mT, (b) γ_0=16% and B=272 mT.

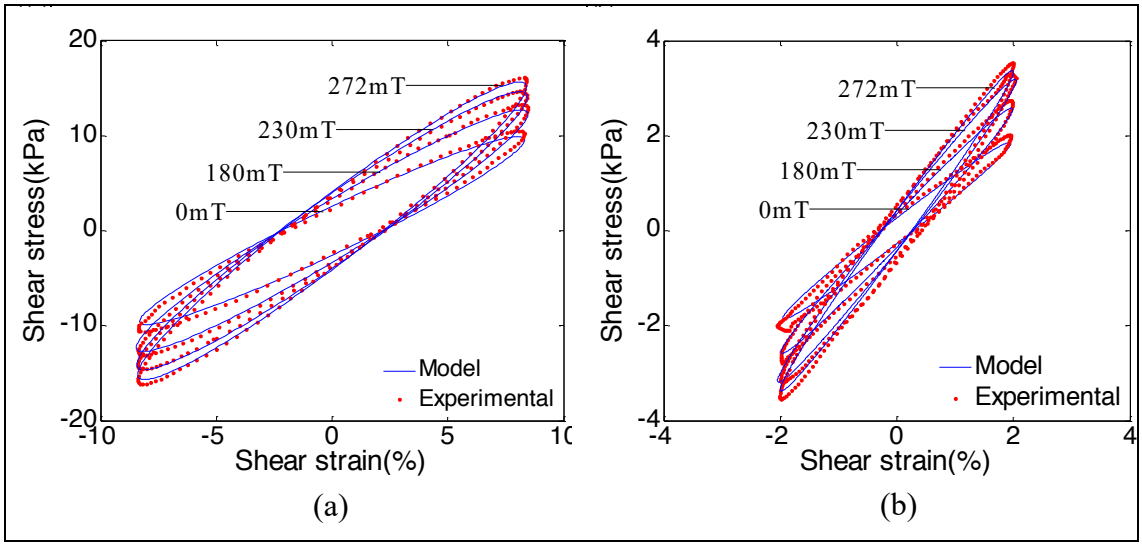

Figure 16. The stress-strain curves of experimental data and proposed model for different magnetic fields. (a) γ_0=8% and f=5 Hz, (b) γ_0=2% and f=0.5 Hz.

Based on the equations (7) and (9), shear storage modulus (G') and loss factor (ζ) can be predicted. Figure 17 shows the relationships of shear storage modulus (G') and loss factor (ζ) with magnetic flux density. By increasing the magnetic flux density both the shear storage modulus (G') and loss factor (ζ) are increased. This behavior is observed for all strain and frequency values. For instance, at the strain of 4% and frequency of 8 Hz the shear storage modulus (G') is increased from 131.4 kPa to 208.2 kPa, more than 50% increment, which illustrates that MRE has variable stiffness behavior. Moreover, the relationship of shear storage modulus (G') and loss factor (ζ) with frequency is shown in Figure18. It can be seen that model prediction for shear storage modulus (G') is quite good.

However, proposed model could not capture the loss factor (ζ) very well. It is because of that the loss factor (ζ) has different variations in frequency range less than 1 Hz and more than 1 Hz. Furthermore, the effect of strain on shear storage modulus (G') and loss factor (ζ) is shown in Figure 19. By increasing the strain, the shear storage modulus (G') is reduced while, the loss factor (ζ) does not change effectively, which both these trends are estimated by developed viscoelastic model very well.

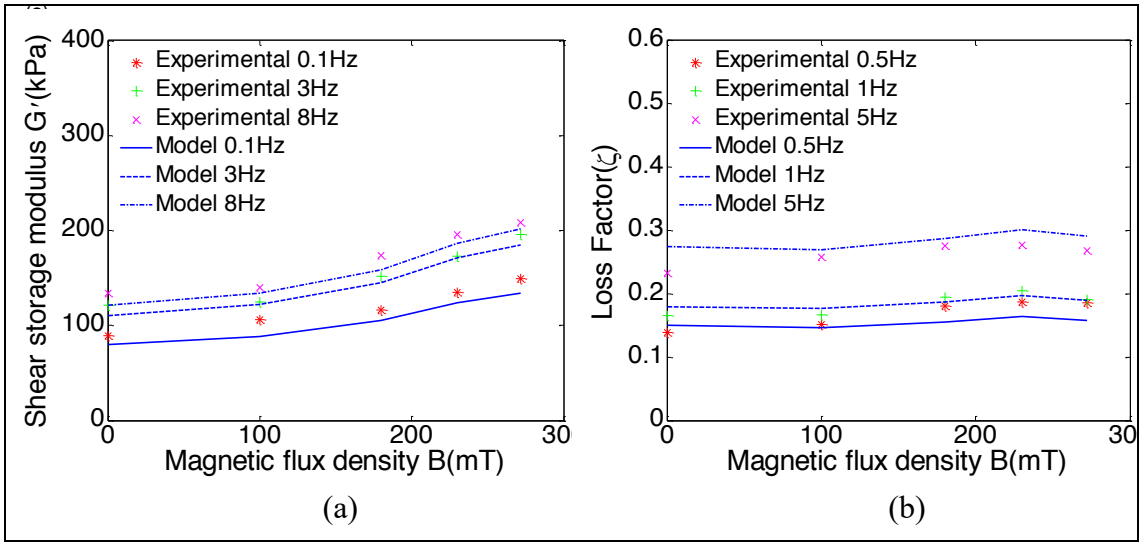

Figure 17. The relationship of storage modulus and loss factor with magnetic flux density.
(a) Shear storage modulus (G')at γ_0=4%, (b) Loss factor (ζ) at γ_0=16%.

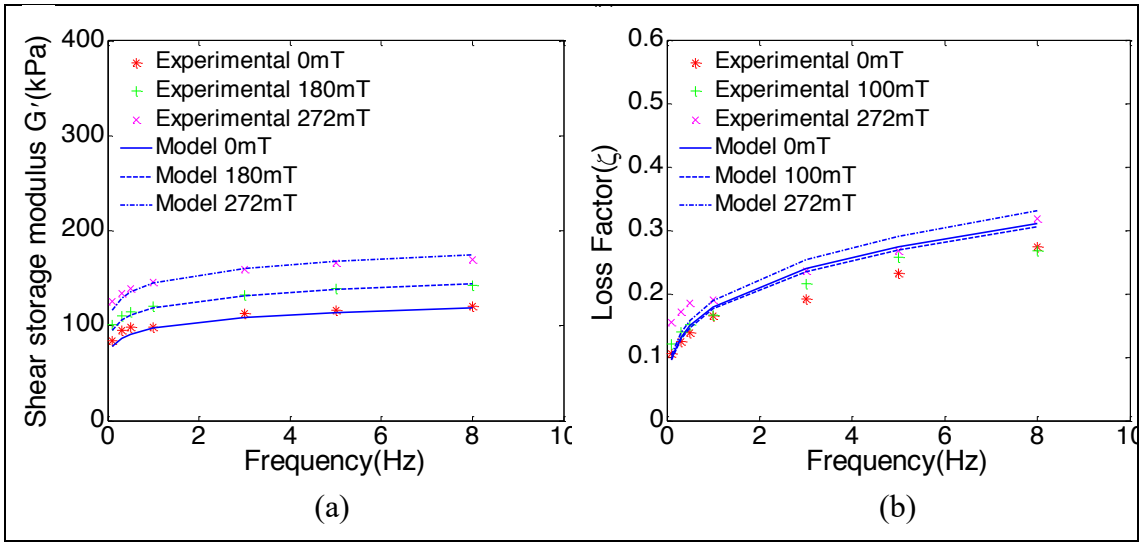

Figure 18. The relationship of storage modulus and loss factor with frequency. shear storage modulus (G') at γ_0=16%, (b) Loss factor (ζ) at γ_0=16%.

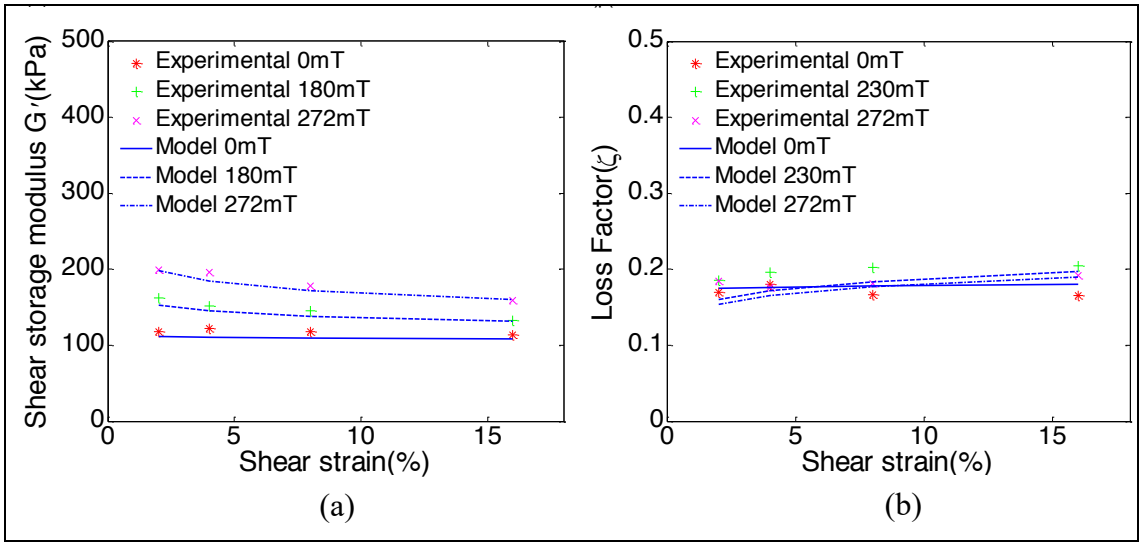

Figure 19. The relationship of storage modulus and loss factor with strain. (a) Shear storage modulus (G') at f=3 Hz, (b) Loss factor (ζ) at f=0.1 Hz.

Table 3. Fitness value of proposed model**.**

Magnetic flux density (0 mT)				
Freq. (Hz)	$\gamma_0 = 2\%$	$\gamma_0 = 4\%$	$\gamma_0 = 8\%$	$\gamma_0 = 16\%$
0.1	85.13	87.65	90.69	92.49
0.3	91.46	88.03	86.26	90.93
0.5	87.26	88.85	92.44	92.34
1	90.03	90.22	91.41	93.14
3	92.03	90.81	87.91	90.04
5	88.44	90.41	92.83	93.56
8	88.35	89.14	91.84	93.99
Magnetic flux density (100 mT)				
0.1	85.26	89.35	87.59	86.36
0.3	88.18	92.25	89.66	94.98
0.5	93.69	91.86	92.52	95.18
1	93.97	96.45	94.43	93.8
3	90.32	92.65	95.03	96.34
5	89.98	94.75	94.03	93.77
8	92.99	93.37	93.16	93.23
Magnetic flux density (180 mT)				
0.1	86.35	88.2282	90.09	93.37
0.3	87.93	87.45	94.66	91.37
0.5	91.9	92.7	94.75	97.42
1	91.04	94.48	94.71	95.55
3	91.8	93.36	95.31	95.01
5	93.72	93.31	94.09	95.87
8	92.65	94.63	95.18	94.62
Magnetic flux density (230 mT)				
0.1	87.97	90.82	92.49	95.06
0.3	93.72	93.42	95.79	93.53
0.5	95.93	95.39	96.29	97.82
1	97.09	94.32	94.58	95.23
3	92.25	96.82	96.39	94.78
5	96.26	97.37	98.54	92.98
8	94.21	97.05	93.91	90.49
Magnetic flux density (272 mT)				
0.1	88.21	87.28	88.19	91.52
0.3	86.63	93.12	91.33	96.78
0.5	95.93	93.03	93.43	96.79
1	95.81	93.78	94.62	94.94
3	92.65	94.12	96.05	93.44
5	92.28	92.31	87.9	94.83
8	93.88	92.03	98.09	90.97

Calculating the fitness value of proposed model

The comparison of experimental data and proposed model is evaluated by Figures 14 to 19. In addition to graphical analogy, the operation of the present model is investigated through a quantitative survey for all experiment cases such as different magnetic flux densities, frequencies and displacement amplitudes. The normalized root mean square function is implemented to calculate fitness value by the following equation:

$$fitness\,value\,(\%) = 100 \times \left[1 - \frac{norm\,(\tau_{Model} - \tau_{Exp})}{norm\,(\tau_{Exp} - mean\,(\tau_{Exp}))} \right] \qquad (14)$$

The fitness values are calculated and prepared in table 3. In the most experimental cases, the fitness values are higher than 90 % and some cases are more than 95% (Perfect fitness). The range of fitness value is from 85.13 % to 98.54 % and the average of fitness value is 93.07 %. Based on the Table 3, it is obvious that for low frequency and low displacement amplitude, the performance of the proposed model is not very well.

Conclusions

This paper proposed a new phenomenological model based on modified Kelvin-Voigt viscoelastic model describing the dynamic behavior of an isotropic MRE in shear mode.

Different sets of double lap shear-loading test are conducted. Especially, dependence of MRE shear storage modulus (G') and loss factor (ζ) to variation of magnetic flux density, loading frequency and strain are experimentally examined. The experimental results show that the proposed model with ten constant coefficients could capture dynamic behavior of the MRE very accurately, regardless of variation in values of parameters such as magnetic flux density, loading frequency and strain. Furthermore, the proposed model estimated the behavior of shear storage modulus (G') precisely in a wide frequency range from 0.1 Hz to 8 Hz, which is nonlinear. The experimental results showed that the tested MRE material possesses both dynamic stiffness and dynamic damping that are controllable through an applied magnetic field. Moreover, the dynamic behavior of MRE is affected by loading condition (input frequency and strain). Based on the experimental results, the following conclusions are obtained.

(1) The shear storage modulus of the tested MRE is a function of magnetic-field intensity and input frequency as well as strain. The storage modulus is enhanced by increasing both the magnetic-field intensity and input frequency and decreases by increasing strain. However, the trend of variation of (G') is not same. The incrementing of shear storage modulus is modeled by third-degree polynomial function of magnetic flux density over the range of tested loading conditions while it increases with input frequency as a power function with the positive power of less than one. Additionally, the value of shear storage modulus reduces by

increasing strain that is predicted by a power function with the negative power of less than one.

(2) The loss factor of tested MRE is relied on the strength of applied magnetic field and input frequency and it is independent of strain, approximately. The loss factor increases linearly by increasing the magnetic flux density while it shows twofold behavior with regard to input frequency. So that, it increases exponentially up to 1 Hz and then increases almost linearly by increasing input frequency. However, the strain does not affect the loss factor effectively.

(3) The results show that the proposed model is in accord with experimental data very well, indicate that the proposed mathematical model is applicable to simulate dynamic behavior of MRE, and it is suitable for control analysis of MRE devices.

References

Bai X-X and Wereley NM. (2014) Magnetorheological impact seat suspensions for ground vehicle crash mitigation. 90570R-90570R-90512.

Behrooz M, Wang X and Gordaninejad F (2014a) Modeling of a new semi-active/passive magnetorheological elastomer isolator. *Smart Materials and Structures* 23(4): 045013.

Behrooz M, Wang X and Gordaninejad F (2014b) Performance of a new magnetorheological elastomer isolation system. *Smart Materials and Structures* 23(4): 045014.

Blom P and Kari L (2005) Amplitude and frequency dependence of magneto-sensitive rubber in a wide frequency range. *Polymer Testing* 24(5): 656-662.

Blom P and Kari L (2011) A nonlinear constitutive audio frequency magneto-sensitive rubber model including amplitude, frequency and magnetic field dependence. *Journal of Sound and Vibration* 330(5): 947-954.

Carlson JD and Jolly MR (2000) MR fluid, foam and elastomer devices. *Mechatronics* 10(4–5): 555-569.

Chen L, Gong X-l and Li W-h (2008) Damping of magnetorheological elastomers. *Chinese Journal of Chemical Physics* 21(6): 581-585.

Chen L, Gong XL and Li WH (2007) Microstructures and viscoelastic properties of anisotropic magnetorheological elastomers. *Smart Materials and Structures* 16(6): 2645-2650.

Danas K, Kankanala SV and Triantafyllidis N (2012) Experiments and modeling of iron-particle-filled magnetorheological elastomers. *Journal of the Mechanics and Physics of Solids* 60(1): 120-138.

Davis LC (1999) Model of magnetorheological elastomers. *Journal of Applied Physics* 85(6): 3348.

Deng H-x, Gong X-l and Wang L-h (2006) Development of an adaptive tuned vibration absorber with magnetorheological elastomer. *Smart Materials and Structures* 15(5): N111-N116.

Dongkyu L, Moonchan L, Namchul J, et al. (2014) Modulus-tunable magnetorheological elastomer microcantilevers. *Smart Materials and Structures* 23(5): 055017.

Du H, Li W and Zhang N (2011) Semi-active variable stiffness vibration control of vehicle seat suspension using an MR elastomer isolator. *Smart Materials and Structures* 20(10): 105003.

Eem S-H, Jung H-J and Koo J-H (2012) Modeling of magneto-rheological elastomers for harmonic shear deformation. *Magnetics, IEEE Transactions on* 48(11): 3080-3083.

Farshad M and Le Roux M (2004) A new active noise abatement barrier system. *Polymer Testing* 23(7): 855-860.

Galipeau E and Ponte Castañeda P (2013) A finite-strain constitutive model for magnetorheological elastomers: Magnetic torques and fiber rotations. *Journal of the Mechanics and Physics of Solids* 61(4): 1065-1090.

Gong XL, Zhang XZ and Zhang PQ (2005) Fabrication and characterization of isotropic magnetorheological elastomers. *Polymer Testing* 24(5): 669-676.

Gordaninejad F, Saiidi M, Hansen BC, et al. (1998) Control of bridges using magnetorheological fluid (MRF) dampers and a fiber-reinforced composite-material column. 2-11.

Guo HT and Liao WH (2012) A novel multifunctional rotary actuator with magnetorheological fluid. *Smart Materials and Structures* 21(6): 065012.

Hu G, Guo M, Li W, et al. (2011) Experimental investigation of the vibration characteristics of a magnetorheological elastomer sandwich beam under non-homogeneous small magnetic fields. *Smart Materials and Structures* 20(12): 127001.

HU W and WERELEY NM (2005) MAGNETORHEOLOGICAL FLUID AND ELASTOMERIC LAG DAMPER FOR HELICOPTER STABILITY AUGMENTATION. *International Journal of Modern Physics B* 19(07n09): 1471-1477.

Kallio M (2005) *The elastic and damping properties of magnetorheological elastomers*: VTT Technical Research Centre of Finland.

Kallio M, Lindroos T, Aalto S, et al. (2007) Dynamic compression testing of a tunable spring element consisting of a magnetorheological elastomer. *Smart Materials and Structures* 16(2): 506-514.

Kavlicoglu BM, Gordaninejad F, Evrensel CA, et al. (2002) High-torque magnetorheological fluid clutch. *SPIE's 9th Annual International Symposium on Smart Structures and Materials.* International Society for Optics and Photonics, 393-400.

Leblanc JL (2002) Rubber–filler interactions and rheological properties in filled compounds. *Progress in Polymer Science* 27(4): 627-687.

Li J, Li Y, Li W, et al. (2013a) Development of adaptive seismic isolators for ultimate seismic protection of civil structures. *SPIE Smart Structures and Materials+ Nondestructive Evaluation and Health Monitoring.* International Society for Optics and Photonics, 86920H-86920H-86912.

Li W, Kostidis K, Zhang X, et al. (2009) Development of a force sensor working with MR elastomers. *Advanced Intelligent Mechatronics, 2009. AIM 2009. IEEE/ASME International Conference on.* IEEE, 233-238.

Li W and Zhang X (2008) Research and applications of MR elastomers. *Recent Patents on Mechanical Engineering* 1(3): 161-166.

Li WH, Zhang XZ and Du H (2013b) Magnetorheological Elastomers and Their Applications. In: Visakh PM, Thomas S, Chandra AK, et al. (eds) *Advances in Elastomers I.* Springer Berlin Heidelberg, 357-374.

Li WH, Zhou Y and Tian TF (2010) Viscoelastic properties of MR elastomers under harmonic loading. *Rheologica Acta* 49(7): 733-740.

Li Y and Li J. (2013) Development and Modeling of a Highly-Adjustable Base Isolator Utilizing Magnetorheological Elastomer. *ASME 2013 Conference on Smart Materials, Adaptive Structures and Intelligent Systems.* American Society of Mechanical Engineers, V001T003A010-V001T003A010.

Li Y, Li J, Li W, et al. (2014) A state-of-the-art review on magnetorheological elastomer devices. *Smart Materials and Structures* 23(12): 123001.

Li Y, Li J, Li W, et al. (2013c) Development and characterization of a magnetorheological elastomer based adaptive seismic isolator. *Smart Materials and Structures* 22(3): 035005.

Li Y, Li J, Tian T, et al. (2013d) A highly adjustable magnetorheological elastomer base isolator for applications of real-time adaptive control. *Smart Materials and Structures* 22(9): 095020.

Lokander M and Stenberg B (2003) Improving the magnetorheological effect in isotropic magnetorheological rubber materials. *Polymer Testing* 22(6): 677-680.

Ngatu GT, Hu W, Wereley NM, et al. (2010) Adaptive Snubber-Type Magnetorheological Fluid-Elastomeric Helicopter Lag Damper. *AIAA Journal* 48(3): 598-610.

Ngatu GT, Wereley NM and Kothera CS (2012) Hydromechanical Analysis of a Fluid-Elastomeric Lag Damper Incorporating Temperature Effects. *Journal of Aircraft* 49(5): 1212-1221.

Payne AR and Whittaker RE (1971) Low Strain Dynamic Properties of Filled Rubbers. *Rubber Chemistry and Technology* 44(2): 440-478.

Raja P, Wang X and Gordaninejad F. (2010) Performance of a high-force controllable MR fluid damper-liquid spring suspension systems. 764311-764311-764318.

Shen Y, Golnaraghi MF and Heppler GR (2004) Experimental Research and Modeling of Magnetorheological Elastomers. *Journal of Intelligent Materials Systems and Structures* 15(1): 27-35.

Stepanov GV, Abramchuk SS, Grishin DA, et al. (2007) Effect of a homogeneous magnetic field on the viscoelastic behavior of magnetic elastomers. *Polymer* 48(2): 488-495.

Sun SS, Chen Y, Yang J, et al. (2014) The development of an adaptive tuned magnetorheological elastomer absorber working in squeeze mode. *Smart Materials and Structures* 23(7): 075009.

W.P. Fletcher ANG (1953) Non-linearity in the dynamic properties of vulcanised rubber compounds. *Transactions of the Institution of the Rubber* 29: 266-280.

Wang K-W, Vavreck AN and Ho C-H (2005) <title>Characterization of a commercial magnetorheological brake/damper in oscillatory motion</title>. 5760: 256-267.

Wang Y, Hu Y, Gong X, et al. (2007) Preparation and properties of magnetorheological elastomers based on silicon rubber/polystyrene blend matrix. *Journal of Applied Polymer Science* 103(5): 3143-3149.

Wen Y-K (1976) Method for random vibration of hysteretic systems. *Journal of the Engineering Mechanics Division* 102(2): 249-263.

Wu J, Gong X, Fan Y, et al. (2010) Anisotropic polyurethane magnetorheological elastomer prepared throughin situpolycondensation under a magnetic field. *Smart Materials and Structures* 19(10): 105007.

Yang G, Spencer Jr BF, Carlson JD, et al. (2002) Large-scale MR fluid dampers: modeling and dynamic performance considerations. *Engineering Structures* 24(3): 309-323.

Yang J, Du H, Li W, et al. (2013) Experimental study and modeling of a novel magnetorheological elastomer isolator. *Smart Materials and Structures* 22(11): 117001.

Yang J, Sun S, Du H, et al. (2014) A novel magnetorheological elastomer isolator with negative changing stiffness for vibration reduction. *Smart Materials and Structures* 23(10): 105023.

Ying Z, Ni Y and Sajjadi M (2013) Nonlinear dynamic characteristics of magneto-rheological visco-elastomers. *Science China Technological Sciences* 56(4): 878-883.

York D, Wang X and Gordaninejad F (2007) A New MR Fluid-Elastomer Vibration Isolator. *Journal of Intelligent Material Systems and Structures* 18(12): 1221-1225.

Yu Y, Li Y and Li J. (2014a) A New Hysteretic Model for Magnetorheological Elastomer Base Isolator and Parameter Identification Based on Modified Artificial Fish Swarm Algorithm. *The International Symposium on Automation and Robotics in Construction and Mining (ISARC 2014).* IAARC, Paper ID: 196.

Yu Y, Li Y and Li J. (2014b) A Novel Strain Stiffening Model for Magnetorheological Elastomer Base Isolator and Parameter Estimation Using Improved Particle Swarm Optimization. *6th World Conference on Structural Control and Monitoring.* IASCM, paper ID: 334.

Zhang WHLXZ (2009) Adaptive tuned dynamic vibration absorbers working with MR elastomers. *Smart Structures and Systems* 5: 517-529.

Zhang X, Peng S, Wen W, et al. (2008) Analysis and fabrication of patterned magnetorheological elastomers. *Smart Materials and Structures* 17(4): 045001.

Zhou GY (2003) Shear properties of a magnetorheological elastomer. *Smart Materials and Structures* 12(1): 139.

Zhou GY and Wang Q (2005) Design of a smart piezoelectric actuator based on a magnetorheological elastomer. *Smart Materials and Structures* 14(4): 504-510.

Zhu J-T, Xu Z-D and Guo Y-Q (2012) Magnetoviscoelasticity parametric model of an MR elastomer vibration mitigation device. *Smart Materials and Structures* 21(7): 075034.